Hindawi Publishing Corporation
Journal of Biomedicine and Biotechnology
Volume 2012, Article ID 262741, 6 pages
doi:10.1155/2012/262741

Research Article

In Vivo Visualization of Heterogeneous Intratumoral Distribution of Hypoxia-Inducible Factor-1α Activity by the Fusion of High-Resolution SPECT and Morphological Imaging Tests

Hirofumi Fujii,[1] Masayuki Yamaguchi,[1] Kazumasa Inoue,[1] Yasuko Mutou,[1] Masashi Ueda,[2] Hideo Saji,[2] Shinae Kizaka-Kondoh,[3] Noriyuki Moriyama,[4] and Izumi O. Umeda[1]

[1] *Functional Imaging Division, National Cancer Center Hospital East, Kashiwa 277-8577, Japan*
[2] *Graduate School of Pharmaceutical Sciences, Kyoto University, Kyoto 606-8501, Japan*
[3] *Graduate School of Bioscience and Biotechnology, Tokyo Institute of Technology, Yokohama 226-8503, Japan*
[4] *Research Center for Cancer Prevention and Screening, National Cancer Center, Tokyo 104-0045, Japan*

Correspondence should be addressed to Izumi O. Umeda, ioumeda@east.ncc.go.jp

Received 1 March 2012; Accepted 24 April 2012

Academic Editor: David J. Yang

Purpose. We aimed to clearly visualize heterogeneous distribution of hypoxia-inducible factor 1α (HIF) activity in tumor tissues *in vivo*. *Methods*. We synthesized of ^{125}I-IPOS, a ^{125}I labeled chimeric protein probe, that would visualize HIF activity. The biodistribution of ^{125}I-IPOS in FM3A tumor-bearing mice was evaluated. Then, the intratumoral localization of this probe was observed by autoradiography, and it was compared with histopathological findings. The distribution of ^{125}I-IPOS in tumors was imaged by a small animal SPECT/CT scanner. The obtained *in vivo* SPECT-CT fusion images were compared with *ex vivo* images of excised tumors. Fusion imaging with MRI was also examined. *Results*. ^{125}I-IPOS well accumulated in FM3A tumors. The intratumoral distribution of ^{125}I-IPOS by autoradiography was quite heterogeneous, and it partially overlapped with that of pimonidazole. High-resolution SPECT-CT fusion images successfully demonstrated the heterogeneity of ^{125}I-IPOS distribution inside tumors. SPECT-MRI fusion images could give more detailed information about the intratumoral distribution of ^{125}I-IPOS. *Conclusion*. High-resolution SPECT images successfully demonstrated heterogeneous intratumoral distribution of ^{125}I-IPOS. SPECT-CT fusion images, more favorably SPECT-MRI fusion images, would be useful to understand the features of heterogeneous intratumoral expression of HIF activity *in vivo*.

1. Introduction

It is very important for the optimization of treatments of tumors to evaluate their features. The features of tumors are usually investigated by pathological examination using some pieces of biopsied specimens. But the pathological findings inside the tumor are often heterogeneous. For example, the expression of human epidermal growth factor receptor 2 (HER2) is often heterogeneous in breast cancer tissues [1]. This means that the degree of HER2 expression can be differently diagnosed according to the biopsy site even in the same tumor. Since, the indication of trastuzumab therapy for breast cancer is determined on the basis of the expression of HER2, the indication of this therapy might also be judged differently according to the biopsy site. To resolve this issue, imaging tests would be useful because they can observe the whole of tumors, unlike pathological tests using biopsied specimens.

There are many studies to evaluate the features of tumors using imaging tests. For example, ^{18}F-fluorodeoxyglucose (FDG) positron emission tomography (PET) has been used to observe glucose metabolism in tumors [2]. And this imaging test is now routinely performed in the clinical practice. Although these imaging tests could image the whole

of tumors, they usually failed to visualize the heterogeneity of tumors due to their poor spatial resolution.

But recent advances in imaging devices and image processing methods have enabled to provide excellent images with high spatial resolution. And it has been also reported that the superimposition of images showing functional information on morphological images such as CT and MRI is quite useful to understand the features of tumors [3]. We will be able to investigate heterogeneous features inside tumors more precisely by using these techniques, and the obtained results will contribute to the optimization of cancer therapy.

Tumor hypoxia is one of the main reasons for the resistance to anticancer therapy such as radiotherapy and chemotherapy [4, 5]. The oxygen partial pressure is heterogeneously distributed in tissues since it depends on intratumoral vasculature [6]. It is difficult to diagnose this heterogeneity in oxygen partial pressure in cancer tissues by biopsied specimens. In some studies, oxygen partial pressure in tumors was measured by inserting an oxygen electrode [7]. But this method is rather invasive and not easy to repeat due to patients' pain. It is also difficult to investigate its heterogeneous distribution in the tumor. Therefore, it is expected to visualize the heterogeneous intratumoral distribution of oxygen partial pressure by *in vivo* imaging tests with high spatial resolution.

Although immunohistological staining by pimonidazole is often used in experimental studies, its clinical application is impossible because pimonidazole cannot be injected into humans due to its toxicity.

Overexpression of hypoxia inducible factor (HIF) partially contributes to the resistance to antitumor therapies under hypoxic conditions [8]. We are interested in evaluating HIF activity as a surrogate of direct measuring of oxygen partial pressure. Recently, an idea where HIF activity is evaluated utilizing the stability of oxygen-dependent degradation (ODD) domain in HIF was reported in the field of optical imaging. And HIF activity was successfully visualized using an optical probe obtained by the fusion of ODD and protein transduction domain (PTD) [9, 10]. As the clinical application of optical imaging techniques is quite limited, its translation in the field of nuclear medicine is expected.

Kudo et al. imaged HIF-1-active tumor hypoxia using a similar chimeric protein probe, ^{123}I-IPOS, a conjugate of ^{123}I-labeled 3-iodobenzoyl norbiotinamide (IBB) and a fusion protein consisting of PTD, ODD, and streptavidin (POS) using a planar gamma camera [11, 12]. Although they could image the tumor itself as a mass, it was difficult to visualize the intratumoral heterogeneous distribution of ^{123}I-IPOS due to poor spatial resolution. Recently, we found that intratumoral heterogeneous distribution of radioactive IPOS might be imaged by using a single-photon-emission computed tomography (SPECT) scanner dedicated for small animal imaging, instead of planar gamma camera [13].

In this study, we aimed to clearly visualize heterogeneous intratumoral localization of ^{125}I-IPOS *in vivo* using fusion imaging methods of high-resolution SPECT and morphological imaging tests such as computed tomography (CT) and magnetic resonance imaging (MRI). And we tried to confirm the usefulness of these fusion images in the diagnosis of heterogeneous features inside tumors.

2. Materials and Methods

2.1. Synthesis of ^{125}I-IPOS. POS was overexpressed in *Escherichia coli* and purified, as previously reported [11]. Purified POS was dissolved in Tris-HCl buffer, pH 8.0. Sodium [^{125}I] iodine (629 GBq/mg as I) was purchased from Perkinelmer Japan. 3-Iodobenzoyl norbiotinamine (IBB) was prepared as described previously [14] and labeled with ^{125}I. ^{125}I-IPOS was obtained by the incubation of ^{125}I-IBB and POS for 1 hour. ^{125}I-IPOS was purified using a Sephadex G-50-filled spin column.

2.2. Animal Tumor Model. Five-week-old female C3H/He mice were purchased from Japan SLC (Hamamatsu, Japan). They were kept at 12/12 h dark-light cycles and were fed *ad libitum*. FM3A mouse breast cancer cells (5×10^6 cells) were subcutaneously implanted into a thigh of a mouse. These mice were used for the experiments 2 weeks after the inoculation. Implanted tumors in this model showed good affinity to IPOS in our previous study [13]. All animal experiments were carried out after the approval by the Ethical Committee for Animal Experiments of our institute.

2.3. Biodistribution of ^{125}I-IPOS. ^{125}I-IPOS (2.0 MBq/30 μg/0.2 mL) was intravenously injected into each mouse via its tail vein. The mice were sacrificed 24 hours after the injection because our previous study revealed that ^{125}I-IPOS accumulated well enough for SPECT imaging [11]. Whole-organ specimens were removed immediately and weighed, and their radioactivity was measured by a dose calibrator (IGC-7, Aloka, Tokyo, Japan) or an autowell gamma counter (ARC-380CL, Aloka).

2.4. Immunohistochemistry and Autoradiography of Excised Tumors. ^{125}I-IPOS (2.0 MBq/30 μg/0.2 mL) was intravenously injected into mice via their tail veins. Pimonidazole (60 mg/kg) was intravenously injected into these mice 1 h before the dissection. These mice were sacrificed 24 h after the injection of ^{125}I-IPOS. The excised tumors were embedded in OCT compound (Sakura Finetek Japan, Tokyo, Japan), frozen, and cut into 6 μm thick sections for hematoxylin-eosin (H&E) staining and fluorescent immunostaining of pimonidazole, and 20 μm thick sections for autoradiography (ARG) using a cryomicrotome (CM 3050S, Leica Instruments, Wetzlar, Germany). For fluorescent immunostaining of pimonidazole, FITC-conjugated mouse IgG_1 monoclonal antibody (Chemicon, Temecula, CA, USA) was treated according to the manufacture's protocol for pimonidazole staining. For ARG, the sliced tumor specimens were placed in contact with an imaging plate (MS2040, Fujifilm, Tokyo, Japan), and the exposed imaging plates were analyzed by an FLA-7000 reader (Fujifilm) and Multi-Gause ver. 3.0 software (Fujifilm).

2.5. SPECT/CT Imaging. High dose of ^{125}I-IPOS (20 MBq/30 μ g/0.2 mL) was intravenously injected into 2 mice via their tail veins. The mice were anesthetized by the inhalation of isoflurane gas 24 hours after the injection. SPECT images were obtained using a SPECT/CT combined scanner dedicated for small animal imaging (NanoSPECT/CT, Bioscan, Washington, D.C., USA). This scanner had 4 detectors with tungsten multipinhole collimators (number of pinholes: 9, the diameter of pinhole: 1.4 mm). First, CT images were acquired by a continuous helical scanning method. The acquisition conditions were as follows: tube voltage: 45 keV, tube current: 177 μA. Then, SPECT images were obtained by a step-and-shoot helical scanning method. The energy window was set between 20 and 36 keV. The acquisition time was set to 5 min for each step. Six steps of 4 detectors, total 24 steps, covered 360 degrees.

The acquired image data of both CT and SPECT were reconstructed by using InVivoScope software (Bioscan). Filtered back-projection algorithms and ordered subset-expectation maximization ones were used for CT image data and for SPECT ones, respectively.

The excised tumor was also imaged using the same SPECT/CT scanner *ex vivo*. The SPECT acquisition time for single step was set to 10 min. Both *in vivo* and *ex vivo* SPECT images superimposed on CT images were compared with each other.

2.6. MR Imaging and Image-Fusion of SPECT and MRI. High-dose ^{125}I-IPOS (20 MBq/30 μg/0.2 mL) was intravenously injected into 2 mice via their tail veins. The mice were anesthetized by mixed gas of isoflurane and nitrogen oxide 24 hours after the injection. After the anesthesia, the mice were put on the special bed that was designed for the fusion imaging of SPECT and MR imaging and immobilized by fastening their extremities to the bed. MR images were acquired using a 3.0T whole-body scanner (Signa HDx, GE Healthcare, Milwaukee, WI, USA) combined with a 3-turn solenoid coil with the internal diameter of 35 mm. The following pulse sequence of 2D fast spin echo was used: TR = 4,000 ms, effective TE = 60.7 ms, echo train length = 8. Field of view was set to $4 \times 4\,\text{cm}^2$ with the matrix size of 256×192. Slice thickness was set to 1 mm. And the total acquisition time was 6 m 40 s. SPECT images were acquired as described above.

SPECT images were superimposed on obtained MR images so that images of markers attached on the cover of the special bed completely overlapped each other on both images.

3. Results

3.1. Biodistribution of ^{125}I-IPOS. The biodistribution of ^{125}I-IPOS in FM3A-bearing mice 24 h after the injection is shown in Figure 1.

^{125}I-IPOS was well accumulated in FM3A tumors implanted in the thigh of mice. The uptake ratio of ^{125}I-IPOS in FM3A tumors was 4.3 ± 0.68% of administered dose/g (mean SD) The reticuloendothelial organs such as liver and spleen showed strong uptake of this probe whereas neck including thyroid gland and muscle showed weak uptake. As a result, tumor-to-blood ratio was as high as 13.1.

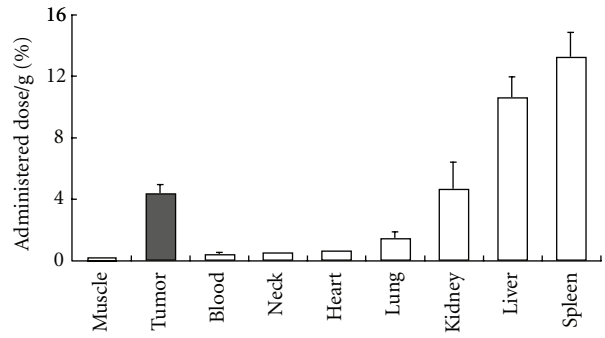

Figure 1: Biodistribution of ^{125}I-POS in FM3A-bearing mice. Administration dose of ^{125}I-POS 2.0 MBq, POS: 30 μg, tumor weight: 0.3–2.3 g, tumor uptake 4.3% AD/g, T/B: 13.1%($n = 5$).

3.2. Immunohistochemistry and Autoradiography of Excised Tumors. ARG tests revealed the heterogeneous ^{125}I-IPOS distribution in FM3A tumors (Figure 2). Fusion imaging of ARG and H&E staining indicated that ^{125}I-IPOS was distributed in viable areas. Fusion imaging of ARG and pimonidazole staining showed the intratumoral location of ^{125}I-IPOS partially overlapped with that of pimonidazole (arrows, Figure 2). But there was discrepancy between the intratumoral location of ^{125}I-IPOS and pimonidazole.

3.3. SPECT/CT Images of FM3A Tumors. As high radioactivity must be accumulated in target tissues to obtain images with excellent spatial resolution, ^{125}I-IPOS with high radioactivity of 22 MBq was administered to each mouse, and *in vivo* SPECT/CT images were acquired. The obtained SPECT images successfully depicted the heterogeneous distribution of ^{125}I-IPOS in FM3A tumors with excellent resolution (Figure 3).

After the acquisition of *in vivo* SPECT images, tumors were excised and weighed and their radioactivity was measured. The radioactivities of both tumors were 0.68 MBq (0.93 g, 0.73 MBq/g) and 1.19 MBq (1.37 g, 0.87 MBq/g), respectively. Then *ex vivo* tumor images were obtained. As *ex vivo* images were obtained with longer acquisition time than *in vivo* ones and there were no surrounding tissues around the tumor tissues that cause scattering of emitted photons in *ex vivo* images, image quality of *ex vivo* images was superior to that of *in vivo* ones. However, *in vivo* images also rather well depicted the heterogeneous intratumoral distribution of ^{125}I-IPOS (Figure 3).

As for the fusion imaging of SPECT and CT, since the tissue contrast inside tumors on CT images was poor, fusion images failed to provide useful information about the features of uptake sites of ^{125}I-POS.

3.4. Fusion Images of SPECT and MRI. MR images could provide more detailed tissue contrast than CT images. As

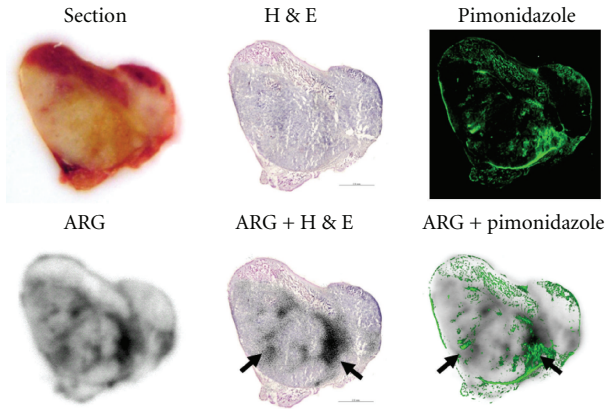

Figure 2: Intratumoral distribution of ^{125}I-POS, pimonidazole. Administration dose of ^{125}I-POS 2.0 MBq, POS: 30 μg, tumor weight: 0.3 g, tumor uptake 5.2%, slice thickness for ARG 20 μm, slice thickness for staining 6 μm.

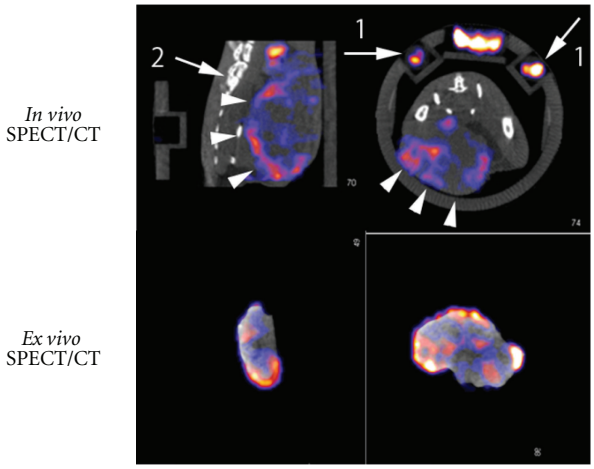

Figure 3: *In vivo* visualization of heterogeneous intratumoral distribution of POS by SPECT/CT. The comparison of *in vivo* SPECT images and *ex vivo* images. Upper raw: *in vivo* SPECT images, lower raw: *ex vivo* SPECT images, left column: sagittal sectional images, right column: axial sectional images. Arrows 1: markers for coregistration, arrows 2: vertebrae, and arrowheads: the tumor.

a result, the superimposition of SPECT images on MR images could give more information about the intratumoral distribution of ^{125}I-IPOS than that on CT images. Figure 4 shows the fusion images of ^{125}I-IPOS SPECT and MR images. As MR images are T2-weighted ones, high signal in the central area of the tumor suggests nonviable tumor tissues. And ^{125}I-IPOS does not accumulate in these high signal areas. SPECT-MR fusion images show that ^{125}I-IPOS is heterogeneously distributed in the low-signal area in the tumor, probably viable tumor areas.

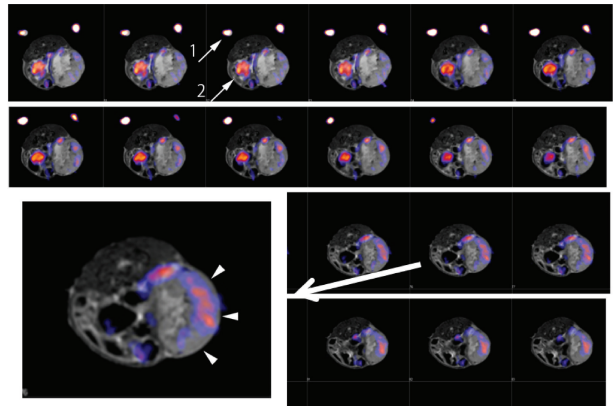

Figure 4: *In vivo* fusion imaging of intratumoral distribution of ^{125}I-POS and MR images. A representative image is enlarged. Arrows 1: markers, arrows 2: urinary bladder, and arrowheads: the tumor.

4. Discussion

We have investigated the precise evaluation of intratumoral localization of HIF activity to establish strategies to optimize cancer treatment.

As the intratumoral distribution of ^{125}I-POS evaluated by ARG partially corresponded with that of pimonidazole, the accumulation of ^{125}I-POS in tumor tissues would be related with tumor hypoxia. The discrepancy can be explained by the facts that HIF activates in the milder hypoxic areas, compared with hypoxic areas with high affinity to pimonidazole [6]. Currently, some PET probes such as ^{18}F-fluoromisonidazole (FMISO), ^{18}F-fluoro-azomycinarabino-furanoside (FAZA), and ^{62}Cu-diacetyl-bis(N4-methylthiosemicarbazone) (ATSM) are under the clinical investigation [4]. As the intratumoral distribution of these probes directly depends on the oxygen partial pressure in tumor tissues, like pimonidazole, they accumulate well in severe hypoxic areas. On the other hand, it is expected that ^{125}I-POS distributes in the tumor according to HIF activity. Our previous study actually demonstrated by an immunohistological method that intratumoral distribution of ^{125}I-IPOS was well correlated with HIF activity [13].

But it is difficult to clearly visualize this heterogeneity in intratumoral localization of ^{125}I-IPOS *in vivo*.

To resolve this difficult problem, we first examined high-resolution SPECT to precisely depict intratumoral distribution of HIF activity. Then, the obtained SPECT images were superimposed on morphological images such as CT and MRI to add anatomical information to intratumoral distribution of HIF activity.

It is necessary to acquire a lot of counts to obtain high-resolution SPECT images [15]. For this purpose, it is required to accumulate high counts of radioactive compounds in target tissues or to acquire images for a long time. The acquisition time is usually limited by effects of longitudinal changes of biodistribution of radioactive compounds and those of the movement of animal bodies. Therefore, it would be better to consider a method to

accumulate a lot of radioactive compounds in target tissues. More accurately speaking, radioactivity concentration in the target tissues should be high.

We synthesized ^{125}I-IPOS with radioactivity concentration of as high as 100 MBq/mL and injected this high activity of ^{125}I-IPOS (20 MBq/30 μg/0.2 mL) into tumor-bearing mice. As a result, ^{125}I-IPOS could be accumulated in tumor tissues with average radioactivity concentration of 0.8 MBq/g. When these mice were acquired by a SPECT scanner dedicated for small animal imaging, heterogeneous intratumoral distribution of ^{125}I-IPOS was successfully imaged *in vivo* with the total acquisition time of 30 minutes.

After that, *ex vivo* SPECT images of excised tumors were obtained. In *ex vivo* imaging, acquisition time was longer. And statistical noise is reduced by the suppression of scattering and attenuation of gamma rays due to the removal of tissues surrounding a tumor. That is why the image quality of *ex vivo* SPECT images is likely to be superior to of that *in vivo* ones. Considering these factors, *in vivo* SPECT images were never inferior to *ex vivo* ones in the light of the visualization of intratumoral heterogeneity.

Our previous experimental study using ^{111}In reported that the radioactivity concentration larger than 0.2 MBq/mL was needed to image the heterogeneous distribution of radiopharmaceuticals in tissues [16]. Since the energy of photons emitted from ^{125}I is much lower than that from ^{111}In [17], radioactivity concentration higher than 0.2 MBq/mL would be required to depict the heterogeneous distribution in tissues by ^{125}I-labeled compounds. The radioactivity concentration of 0.8 MBq/g, which we obtained in this study, was high enough to visualize the heterogeneous distribution of ^{125}I-labeled compounds.

In the light of the energy of emitted photons and half-life, ^{123}I-labeled compounds are more suitable for clinical nuclear medicine tests than ^{125}I ones. But, to obtain SPECT images with excellent spatial resolution in small animal studies, radioactive probes with high radioactive concentration and specific radioactivity are required [16]. In our country, it is, however, very difficult to get Na^{123}I with high specific radioactivity. That is why we used ^{125}I-labeled compounds in this study.

It is often difficult to evaluate the features of target tissues where radioactive compounds accumulated only by SPECT images due to the lack of anatomical information. The situation is same in the clinical practice. Therefore, superimposition of SPECT images on morphological images such as CT and MRI is actively examined to settle this problem.

In this study, as images of ^{125}I-IPOS were obtained using a SPECT/CT combined scanner, the fusion images of SPECT and CT could be easily obtained using preinstalled software. The superimposition on CT images provided the information about the position of the uptake of ^{125}I-IPOS. But additional information about the pathological features of ^{125}I-IPOS uptake areas was poor because the tissue contrast of CT images was not excellent and the change of CT number inside tumors was minimal.

On the other hand, fusion imaging of SPECT and MRI took a lot of effort. As MR images could not be obtained using a combined scanner with SPECT, it was required to image mice by putting them on a special bed with markers for coregistration [18]. Good tissue contrast of MRI, however, could provide important information about the features of tumor interiors. In this study, SPECT-MRI fusion images successfully suggested that ^{125}I-IPOS was distributed in mainly viable tumor tissues.

There are some problems that must be settled in SPECT-MRI fusion imaging: the accuracy of coregistration, the distortion of images, and so on. But SPECT-MRI fusion images can provide more useful information about the features of tumor interiors than SPECT-CT images. Therefore, SPECT-MRI fusion imaging should be more actively investigated.

The clinical application of fusion images of radioactive IPOS SPECT and morphological imaging tests, especially MRI, will be an important research project in the future. It is expected that the fusion images of radioactive IPOS SPECT and CT or MRI will contribute toward overcoming the resistance to cancer therapy such as radiotherapy and chemotherapy.

5. Conclusion

High-resolution SPECT images successfully demonstrated heterogeneous intratumoral distribution of ^{125}I-IPOS *in vivo*. The superimposition of SPECT images on CT images, more favorably MR images, would be useful to understand the features of heterogeneous intratumoral expression of HIF activity *in vivo*.

Conflict of Interests

The authors declare no conflict of interests.

Acknowledgments

This study was partially supported by Grants-in-Aid from the Japanese Ministry of Education, Culture, Sports, Science and Technology (MEXT) and the Japan Society for the Promotion of Science (JSPS), Health Labour Sciences Research Grant (Research on 3rd Term Comprehensive 10-year Strategy for Cancer Control) from the Japanese Ministry of Health, Labour and Welfare (MHLW) and the National Cancer Center Research and Development Fund.

References

[1] M. Chivukula, R. Bhargava, A. Brufsky, U. Surti, and D. J. Dabbs, "Clinical importance of HER2 immunohistologic heterogeneous expression in core-needle biopsies vs resection specimens for equivocal (immunohistochemical score 2+) cases," *Modern Pathology*, vol. 21, no. 4, pp. 363–368, 2008.

[2] K. Kubota, "From tumor biology to clinical PET: a review of positron emission tomography (PET) in oncology," *Annals of Nuclear Medicine*, vol. 15, no. 6, pp. 471–486, 2001.

[3] R. L. Wahl, L. E. Quint, R. D. Cieslak, A. M. Aisen, R. A. Koeppe, and C. R. Meyer, "'Anatometabolic' tumor imaging: fusion of FDG PET with CT or MRI to localize foci of increased activity," *Journal of Nuclear Medicine*, vol. 34, no. 7, pp. 1190–1197, 1993.

[4] A. R. Padhani, K. A. Krohn, J. S. Lewis, and M. Alber, "Imaging oxygenation of human tumours," *European Radiology*, vol. 17, no. 4, pp. 861–872, 2007.

[5] P. Vaupel and A. Mayer, "Hypoxia in cancer: significance and impact on clinical outcome," *Cancer and Metastasis Reviews*, vol. 26, no. 2, pp. 225–239, 2007.

[6] S. Kizaka-Kondoh and H. Konse-Nagasawa, "Significance of nitroimidazole compounds and hypoxia-inducible factor-1 for imaging tumor hypoxia," *Cancer Science*, vol. 100, no. 8, pp. 1366–1373, 2009.

[7] J. D. Chapman, "Measurement of tumor hypoxia by invasive and non-invasive procedures: a review of recent clinical studies," *Radiotherapy and Oncology*, vol. 20, no. 1, supplement, pp. 13–19, 1991.

[8] G. L. Semenza, "Intratumoral hypoxia, radiation resistance, and HIF-1," *Cancer Cell*, vol. 5, no. 5, pp. 405–406, 2004.

[9] H. Harada, S. Kizaka-Kondoh, and M. Hiraoka, "Optical imaging of tumor hypoxia and evaluation of efficacy of a hypoxia-targeting drug in living animals," *Molecular Imaging*, vol. 4, no. 3, pp. 182–193, 2005.

[10] T. Kuchimaru, T. Kadonosono, S. Tanaka, T. Ushiki, M. Hiraoka, and S. Kizaka-Kondoh, "In vivo imaging of HIF-active tumors by an oxygen- dependent degradation protein probe with an interchangeable labeling system," *PLoS ONE*, vol. 5, no. 12, article e15736, 2010.

[11] T. Kudo, M. Ueda, Y. Kuge et al., "Imaging of HIF-1-active tumor hypoxia using a protein effectively delivered to and specifically stabilized in HIF-1-active tumor cells," *Journal of Nuclear Medicine*, vol. 50, no. 6, pp. 942–949, 2009.

[12] M. Ueda, T. Kudo, Y. Kuge et al., "Rapid detection of hypoxia-inducible factor-1-active tumours: pretargeted imaging with a protein degrading in a mechanism similar to hypoxia-inducible factor-1α," *European Journal of Nuclear Medicine and Molecular Imaging*, vol. 37, no. 8, pp. 1566–1574, 2010.

[13] M. Ueda, T. Kudo, Y. Mutou et al., "Evaluation of ^{125}I-IPOS as a molecular imaging probe for hypoxia-inducible factor-1-active regions in a tumor: comparison among single-photon emission computed tomography/X-ray computed tomography imaging, autoradiography, and immunohistochemistry," *Cancer Science*, vol. 102, no. 11, pp. 2090–2096, 2011.

[14] C. F. Foulon, K. L. Alston, and M. R. Zalutsky, "Synthesis and preliminary biological evaluation of (3-iodobenzoyl) norbiotinamide and ((5-iodo-3-pyridinyl)carbonyl)norbiotinamide: two Radioiodinated biotin conjugates with improved stability," *Bioconjugate Chemistry*, vol. 8, no. 2, pp. 179–186, 1997.

[15] S. R. Cherry, J. A. Sorenson, and M. E. Phelps, *Image Quality in Nuclear Medicine*, Physics in Nuclear Medicine, Saunders, Philadelphia, Pa, USA, 2003.

[16] I. O. Umeda, K. Tani, K. Tsuda et al., "High resolution SPECT imaging for visualization of intratumoral heterogeneity using a SPECT/CT scanner dedicated for small animal imaging," *Annals of Nuclear Medicine*, vol. 26, no. 1, pp. 67–76, 2012.

[17] F. J. Beekman, D. P. McElroy, F. Berger, S. S. Gambhir, E. J. Hoffman, and S. R. Cherry, "Towards in vivo nuclear microscopy: iodine-125 imaging in mice using micro-pinholes," *European Journal of Nuclear Medicine*, vol. 29, no. 7, pp. 933–938, 2002.

[18] M. Yamaguchi, D. Suzuki, R. Shimizu et al., "Precise co-registration of SPECT and MRI for small animal imaging using a common animal bed with external references: visualization of macrophage distribution within inflammatory lymph nodes," in *Proceedings of 18th Meeting of the International Society for Magnetic Resonance in Medicine*, vol. 3963, 2010.